Generic Roughness Meta-model in 3D Printing by Fused Deposition Modeling

Elnaz Asadollahi-Yazdi, Julien Gardan, Pascal Lafon

RESEARCH PAPER

Generic Roughness Meta-model in 3D Printing by Fused Deposition Modeling

– Elnaz Asadollahiyazdi Julien Gardan Pascal Lafon

ABSTRACT
Design for Additive Manufacturing (DfAM) aims at optimizing the product design based on design rules defined thanks to Additive Manufacturing (AM) constraints. To elaborate a functional design, several parameters like part orientation and layer thickness influence the results of mechanical strength, roughness, and manufacturing time. Surface roughness is an important input of Fused Deposition Modeling which impacts the product functionalities. To participate in product design optimization and DfAM development, this research suggests studying roughness models in order to clarify the best functional design methodology. This analysis permits to propose a meta-model that provides a better estimation for the surface roughness of the FDM products. A new roughness model is developed by a combination of genetic programming and symbolic regression due to the experimental data which helps the manufacturer to predict the surface quality of the products before fabrication. It enables us to estimate the surface roughness of all the AM products fabricated in a different value of layer thickness for all possible orientations in the space regarding part building direction.

KEYWORDS
Additive Manufacturing; Design for Additive Manufacturing; Fused Deposition Modeling; 3D printing; Surface Roughness; Functional design with roughness optimization

1. Introduction

Nowadays, Additive Manufacturing (AM), as one of the nine main pillars of industry 4.0, has revolutionized product development and fabrication (Asadollahi-Yazdi et al. (2020)). It is a new technology to produce different versions of complex products with a material range. Firstly, this manufacturing method was used for Rapid Prototyping but it is currently used in different industrial and educational applications. It includes a group of technologies, like Fused Deposition Modeling (FDM), Selective Laser Sintering (SLS), Selective Laser Melting (SLM), which makes the products layer by layer. These technologies are different in terms of used material, and the process of layer fabrication (Gardan (2016)). This manufacturing builds the products directly from 3D computer-aided design models or reverse-engineering data without conventional tooling or fixture (Asadollahi-Yazdi, Gardan, and Lafon (2018)).

Among AM technologies, FDM is one of the most extensively used AM techniques which has substantially shortened product development time and cost. FDM is a layer AM process that uses a thermoplastic filament, such as ABS (Acrylonitrile Butadiene Styrene) and PLA (Poly-lactic Acid), by fused depositing. The layers are fabricated

by filament extrusion which is extruded by a nozzle. The nozzle contains resistive heaters that keep the plastic at a temperature just above its melting point so that it flows easily through the nozzle and forms the layer. The plastic hardens immediately after flowing from the nozzle and bonds to the layer below. It traces the part's cross-sectional geometry layer by layer, then moving up vertically to repeat the process to produce the layers from down to up for finishing the part fabrication (Gardan (2016)).

This different fabrication process affects the product characteristics which are produced by these technologies. Design for Additive Manufacturing (DfAM), as a concept which focuses on the design of products while considering the additive manufacturing criteria and constraints early in the design process, permits to increase chances of success and shorten the development cycle to have a cost-effective production (Vaneker et al. (2020)). In this concept, it is necessary to evaluate some criteria like mechanical strength, surface quality, etc. before fabrication in order to create the optimal design and manufacturing.

One of the most important characteristics of products is surface roughness that will be presented in the next section. Different models are also presented to predict the surface roughness of the products which will be discussed in this article and finally, a new meta-model based on the experimental data will be proposed for calculating the surface roughness before production. This model permits the users to be sure about satisfying one of the significant manufacturing criteria as surface roughness.

Therefore, the remainder of this paper is organized as follows. The surface roughness of AM products will be discussed in the next section. Then, the different existed models for roughness are discussed in section 3. Section 4 is devoted to the proposed methodology as a new roughness model to estimate surface quality. Finally, section 5 concludes with a summary.

2. Surface roughness in 3D printing

The AM advantages include producing the complex geometries without any additional cost and tooling, etc. encourage the manufacturers to use AM technologies (Asadollahi-Yazdi, Gardan, and Lafon (2016, 2017)) but they have also some disadvantages such as surface quality that is originated from the layer by layer fabrication and the orientation of the part in the build platform.

Surface quality can be measured by surface roughness as R_{a}. As described in ASME B46.1 (Standard (2002)),” R_{a} is the arithmetic average of the absolute values of the profile height deviations from the mean line, recorded within the evaluation length. Simply put, R_{a} is the average of an individual measurement set of surface peaks and valleys.” As a consequence of layered manufacturing, the surface finish of AM parts is excessively rough. Since, this surface roughness has influences on the material functional properties, such as mechanical behavior, optical properties, and frictional behavior. Therefore, it is necessary to control the surface of the AM products (Vahabli and Rahmati (2016b)). Surface roughness (R_{a}) can be defined as Equation (1) (Byun and Lee (2006)):

$$R_{\mathrm{a}} = \frac{1}{l}\int_0^l \mid y(x) - y_c \mid dx \tag{1}$$

Where $y(x)$ is roughness profile value, l is the evaluation length, and y_c is the centerline position. The areas above and below the line are equal. Therefore, R_{a} represents the

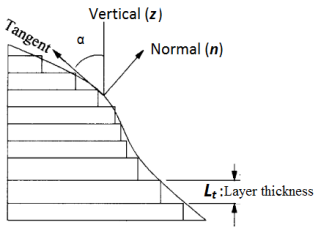

Figure 1. Deposition angle and layer thickness (Pandey, Reddy, and Dhande (2003c))

summation of the areas above and below the line, divided by the evaluation length (Byun and Lee (2006)).

Different methods are used to measure and improve the surface roughness like analysis of different AM parameters effects on surface roughness (Wang et al. (2019); Garg, Singh, and Ahuja (2017); Huang et al. (2019); Pérez et al. (2018); Salokhe and Shaikh (2019); Jain et al. (2020)), Pre-processing and post-processing techniques to enhance surface roughness (Khan and Dash (2019); Mu et al. (2020); Ko and Lee (2017); Boschetto, Bottini, and Veniali (2016); Jayanth, Senthil, and Prakash (2018); Lalegani Dezaki, Mohd Ariffin, and Ismail (2020); Rajan et al. (2020); Singh, Singh, and Boparai (2020)), and mathematical representations and optimization approaches to analyze and improve the surface roughness (Li et al. (2016); Sheoran and Kumar (2019); Cherkia et al. (2020); Nagendra et al. (2020)). Moreover, several models are presented to predict and calculate the surface roughness based on different significant parameters. In the following, these models will be analyzed which allow developing a new meta-model.

3. Different roughness models

In this section, different models of surfacde roughnrss presented by other researchers, will be provided. These various models are provided by consideration of different schematics for the surface profile.

According to several experiments and researches, roughness depends on layer thickness value and orientation types. Producing with the thicker layer (low resolution) increases the roughness values and the surface quality is decreased. Moreover, orientation influences the surface quality due to the angle between the tangent vector of parts and a vertical direction for each orientation. Other parameters affect the surface quality but they have less effect on the roughness value. Therefore, we deal with the different models which calculate the surface roughness based on the layer thickness and orientation will be discussed in this article.

In these models, it is supposed that α, as deposition angle, is a factor to define the orientation types. It is an angle between the tangent vector of parts and vertical direction $\vec{z}$ (see Figure 1). In these formulations, L_t as layer thickness and R_{a} as roughness value are supposed in the union of mm and µm respectively. These models, including theoretical and empirical models, can be replaced by trial-and-error methods to save money and time. A summary of these models is presented as follow:

- **Pandey, Reddy, and Dhande (2003c) model (1):** This semi-empirical model is presented through approximating the layer edge profile by a parabola with base length approximating $(L_t/\cos(90^\circ - \alpha))$ and height as $30-35\%$ of base

length as shown in Figure 2. The mean surface (mm^2) is assumed to be in the middle. The centerline average method is used to evaluate the surface roughness. So, the R_{a} value is obtained as:

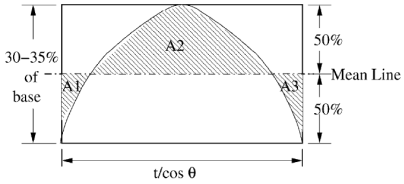

Figure 2. Surface profile approximation (Pandey, Reddy, and Dhande (2003c))

$$R_{\mathrm{a}}(\mu\mathrm{m}) = 1000\frac{(A_1 + A_2 + A_3(mm^2))}{L_t(\mathrm{mm})/\cos(90^\circ - \alpha)} \tag{2}$$

where A_1, A_2, and A_3 are the areas that are illustrated in Figure 2. This model can be written based on the experimental data as Equation (3). This formulation is an approximation estimation by considering a coefficient which is not fixed:

$$R_{\mathrm{a}}(\mu\mathrm{m}) = (71 \sim 93)\frac{L_t}{\cos(90^\circ - \alpha)} \tag{3}$$

- **Pandey, Reddy, and Dhande (2003a) model (2):** An adaptive slicing methodology is presented based on a realistic build edge profile to predict surface roughness. This methodology uses direct slicing and tessellated model (STL) based on two concepts of limiting cusp height and the limited deviation of the cross-sectional area (plane normal to the z-axis) of the part.

$$R_{\mathrm{a}}(\mu\mathrm{m}) = (69.28 - 72.36)\frac{L_t}{\cos(90^\circ - \alpha)} \tag{4}$$

  Furthermore, this formulation (Equation 4) is used to determine the best part orientation according to the facet area by optimizing build time, support structure, and accuracy regarding surface roughness (Pandey, Reddy, and Dhande (2007)).
- **Penday model (3):** Thrimurthulu, Pandey, and Reddy (2004) transformed the Penday models into a simple empirical model. This model is developed by approximation of layer edge profile by a parabola with base length $L_t/\cos(90^\circ - \alpha)$ as Equation (5) (Pandey, Reddy, and Dhande (2003a,b,c); Pandey, Thrimurthulu, and Reddy* (2004); Thrimurthulu, Pandey, and Reddy (2004)). In this formulation, W is dimensionless adjustment parameter for FDM ($W = 0.2$). Also, it is evident that this formulation is an approximate estimation by considering a coefficient which is not fixed. It must be mentioned that $R_{\mathrm{a}}(90, L_t)$ and $R_{\mathrm{a}}(70, L_t)$ are calculated by the same expressions (Equation (5)) for $R_{\mathrm{a}}(\alpha, L_t)$ when $\alpha = 70^\circ, 90^\circ$: This formulation is used by Li et al. (2010) to find the optimal orientation regarding support area, fabrication time, and surface roughness.
- **Byun and Lee (2003) model:** The surface profile is considered symmetric in this model. It is assumed that an inclined surface has sharp edges (see Figure 3).

$$R_{\mathrm{a}}(\alpha, L_t) = \begin{cases} (69.28 \sim 72.36)\frac{L_t(\mathrm{mm})}{\cos(90^\circ - \alpha)} & 0 \le \alpha \le 70^\circ \\ \frac{1}{20}(90R_{\mathrm{a}}(70, L_t) - 70R_{\mathrm{a}}(90, L_t) + \alpha(Ra(90, L_t) - R_{\mathrm{a}}(70, L_t)) & 70^\circ < \alpha < 90^\circ \\ R_{\mathrm{a}} = 112.6L_t & \alpha = 90^\circ \\ R_{\mathrm{a}}(\alpha - 90, L_t)(1 + W) & 90^\circ < \alpha \le 180^\circ \end{cases} \tag{5}$$

$$R_{\mathrm{a}}(\alpha, L_t) = \begin{cases} 0 & \alpha = 0, \frac{\pi}{2}, \pi \\ 1000\frac{L_t}{4} - \frac{(R_1^2 + R_2^2)(1 - \frac{\pi}{4})\sin(90^\circ - \alpha)}{1000L_t} + \frac{\left((R_1^2 - R_2^2)(1 - \frac{\pi}{4})\right)^2}{(1000L_t)^3}\sin(90^\circ - \alpha)\tan(90^\circ - \alpha) & Otherwise \end{cases} \tag{7}$$

The predicted values coming from Equation (6) are obtained and compared with the experimental results. If the surface profile is symmetric, the arithmetic surface roughness must be calculated as set out in Equation (6), where L is range of evaluation which is equal to $L = L_t/\sin(90^\circ - \alpha)$. The proposed model is applied to diverse features of varying sizes in the x, y, and z directions.

$$R_{\mathrm{a}}(\mu\mathrm{m}) = 1000\frac{L_t^2}{L}\frac{\cos(90^\circ - \alpha)}{\sin(90^\circ - \alpha)} \tag{6}$$

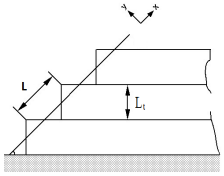

Figure 3. Surface profile of inclined surface (Byun and Lee (2003))

- **Byun and Lee (2006) model:** In this model, the maximum value of R_{a} is defined as Equation (7). Surface roughness of an inclined facet and the contact area of supports are used to estimate the surface quality of a part. In this model, roughness is a function of L_t, α, R_1, and R_2 (Equation (7)). In the case of $\alpha = 0, \frac{\pi}{2}$, and π, it is assumed that R_{a} is zero. In this equation, R_1 is the radius of fillet and R_2 is the corner radius.

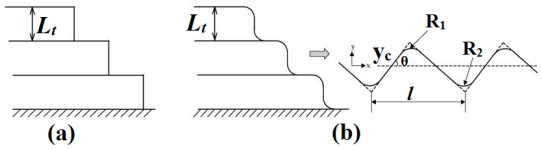

Figure 4. (a) Manufactured surface with sharp edge- (b) with round edge (Byun and Lee (2006))

- **Mason (2006) model:** A multi-axis fused deposition is investigated in this study. This model is written as Equation (8) that is eventually a similar estima-

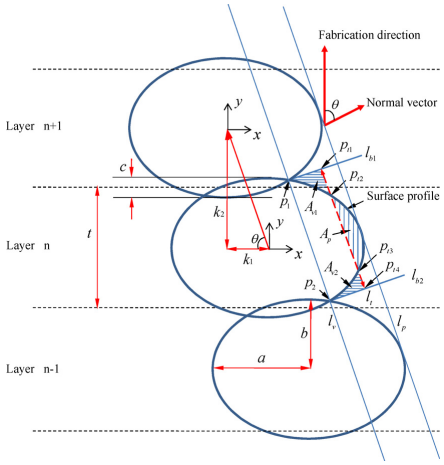

Figure 6. Schematic for modeling the surface profile of the FDM parts (Ahn et al. (2009))

tion proposed by Ahn et al. (2009) with a phase shift (ϕ):

$$R_{\mathrm{a}} = 1000 L_t \cos(90^\circ - \alpha) \tag{8}$$

- **Ahn, Kim, and Lee (2009) model (1):** From the approximated modeling for the stair-stepping effect (see Figure 5), a theoretical distribution model for average surface roughness (R_{a}) can be presented. This model is developed according to the changes in the surface angle which can be expressed by Equation (9) that is coming from interpolation. A and W, shown in Figure 5, are the elements of surface profile schematic. The validation of this methodology is examined by several applications. Therefore, both theoretical and empirical methods are defined in an analytical modeling.

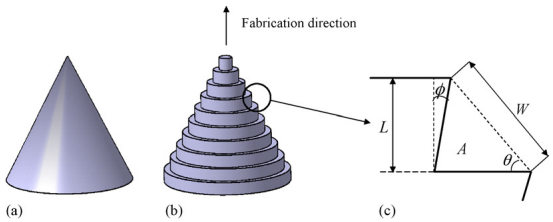

Figure 5. Stair stepping effect- (a) CAD model; (b) AM processed part;(c)Surface profile schematic (Ahn, Kim, and Lee (2009))

$$R_{\mathrm{a}} = 1000 \frac{A}{W} = 1000 \frac{L}{2} \left| \frac{\cos((90 - \alpha) - \phi)}{\cos \phi} \right| \tag{9}$$

Generally, ϕ is defined between 5° and 15°. In this study, it is supposed as an average value equal to 10°.

- **Ahn et al. (2009) model (2):** Surface profile is considered as an elliptical curve which depends on the surface angle, cross-sectional shape, layer thickness, overlap interval, and horizontal interval as air gap in this model.

$$R_{\mathrm{a}} = \frac{A_f}{I} = \frac{A_{f_p} + A_{f_v}}{\sqrt{(x_1 - x_2)^2 + (y_1 - y_2)^2}} \tag{10}$$

In this equation, A_f as the final computed area is determined by moving the temporary center-line and I is the distance between two boundary lines (distance between two points of p_1 and p_2) which are demonstrated in Figure 6.

- **Sreedhar, Mathikumar, and Jothi (2012) model:** In this model, the center line average (CLA) method is used to evaluate the surface roughness as Equation (11).

$$R_{\mathrm{a}} = 1000 \frac{L_t \sin \alpha}{4} \tag{11}$$

- **Boschetto, Giordano, and Veniali (2013b) model:** A geometrical model of the deposited filament is developed as shown in Figure 7. In this figure, the planes Γ and Ω are defined perpendicular to the build direction (b) and deposition direction (d), respectively. α is the angle between the part surface and the Ω plane. γ is the angle between the Γ plane and the measurement direction of the profile.

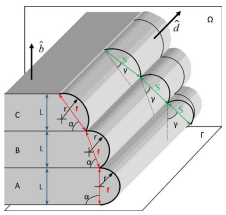

Figure 7. Filament geometry (Boschetto, Giordano, and Veniali (2013b))

It is assumed that width and the radius can be calculated according to:

$$r = L_t/2 \csc \alpha \quad f = L_t \csc \alpha \tag{12}$$

Roughness model is provided as Equation (13). Experimental data proved that this model is not reliable for the α less than 30° and greater than 150°.

$$R_{\mathrm{a}} = 1000 L_t \frac{\csc \alpha}{9\sqrt{(3)}} \tag{13}$$

- **Boschetto, Giordano, and Veniali (2013a) model:** Neural network is used to fit experimental data and to find the best formulation by an evaluation function. This formulation is useful for the value of layer thickness between 0.254 and 0.331 mm.

$$\begin{aligned} R_{\mathrm{a}} = -6118 &+ 1766 \tanh[15.67 + 0.016\alpha - 0.049L_t] - 200.4 \tanh[11.54 - 0.08\alpha - 0.045L_t] \\ &- 24.87 \tanh[17.13 - 0.044\alpha - 0.042L_t] - 1131 \tanh[10.33 + 0.019\alpha - 0.034L_t] \\ &+ 5501 \tanh[20.84 - 0.056\alpha - 0.02L_t] - 195.5 \tanh[4.559 + 0.062\alpha - 0.018L_t] \\ &- 101.3 \tanh[20.09 - 0.088\alpha - 0.018L_t] + 116.1 \tanh[21.66 - 0.105\alpha - 0.013L_t] \end{aligned}$$

- **Vahabli and Rahmati (2016a,b) model:** Roughness (R_{a} in µm) is calculated

$$R_{\mathrm{a}}(\alpha, L_t) = \begin{cases} 70\dfrac{L_t}{\cos(\alpha)} & 0 \le \alpha \le 70^\circ \\ 1000 L_t \sin\left(\frac{90^\circ-\alpha}{4}\right)\tan(90^\circ-\alpha) & 70^\circ < \alpha \le 90^\circ \\ 70\dfrac{L_t}{\cos(\alpha-90^\circ)}(1+W) & 90^\circ < \alpha \le 135^\circ \\ 1000\frac{L_t}{4} - \frac{(R_1^2+R_2^2)(1-\frac{\pi}{4})\sin(90^\circ-\alpha)}{1000L_t} + \frac{\left((R_1^2-R_2^2)(1-\frac{\pi}{4})\right)^2}{(1000L_t)^3}\frac{\sin^2(90^\circ-\alpha)}{\cos(90^\circ-\alpha)} & 135^\circ < \alpha < 160^\circ \\ 1000\frac{L_t}{2}\cos(90^\circ-\alpha) & 160^\circ \le \alpha \le 180^\circ \end{cases} \tag{14}$$

Table 1. Experimental analysis details

Specimen	Material	Machine Model	Measurement machine	Details	Research
a	ABS	Stratasys,Dimension BST 768	Taylor-Hobson Form Talysurf Plus	$L_t = 0.254\,\mathrm{mm}$	Boschetto, Giordano, and Veniali (2013a)
	ABS plus	Stratasys,Fortus 400			
	ULTEM 9085	Stratasys,Fortus 400			
	Poly carbonate	Stratasys,Fortus 360			
b	ABS	Stratasys, MAXUM	Surftest Formtracer	$L_t = 0.178\,\mathrm{mm}, \alpha_{step} = 3^\circ$	Ahn et al. (2009)
	ABS	Stratasys, MAXUM	Surftest Formtracer	$L_t = 0.254\,\mathrm{mm}, \alpha_{step} = 3^\circ$	Ahn, Kwon, and Lee (2008)
	ABSplus	Stratasys, Dimension SST 1200es	MahrSurf MFW250	$L_t = 0.3302\,\mathrm{mm}, \alpha_{step} = 5^\circ$	Vahabli and Rahmati (2016b)
	ABS-M30	FDMFortus 400mc	Rugosurf 10G surface tester	$L_t = 0.178, 0.254\,\mathrm{mm}, \alpha_{step} = 5^\circ$	Taufik and Jain (2016)
c	ABS	Stratasys, FDM 8000	wavelength cut-off	$L_t = 0.25\,\mathrm{mm}$	Byun et al Byun and Lee (2006)

through a hybrid estimation methodology. Vahabli and Rahmati (2016a,b) proposed this estimation by comparison of experimental data obtained in Vahabli and Rahmati (2016a) and the other existed models (Mason (2006); Byun and Lee (2006); Ahn, Kwon, and Lee (2008); Pandey, Reddy, and Dhande (2003c)) to find the roughness for different values of deposition angles (α). In this formulation (Equation (14)), W is the fixed dimensionless adjustment parameter for supported facets in roughness calculation that is supposed equal to 0.2 for all FDM systems based on an experimentally measured surface roughness by Reddy and Pandey (2005) for the supported area. $R_1 = 0.045$ and $R_2 = 0.01$ are the radius of fillet and corner respectively.

To validate the proposed approach by researchers, the practical data is gathered through the measurement of surface roughness of the parts fabricated by FDM. A summary of these experimental analyses is described in Table 1. This table contains different experiments that perform on several types of specimens, which are different in terms of geometry, material, machine, measurement instrument, and layer thickness values. These specimens categorized as types of "a" to "c" as illustrated in Figure 8.

To analyze and compare these models with experimental results, the models are

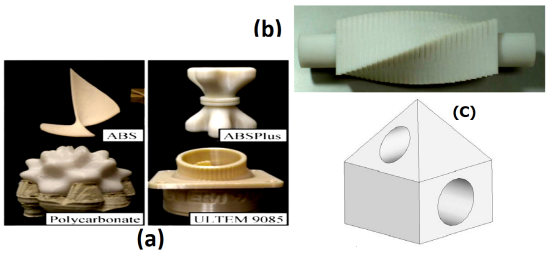

Figure 8. Different specimens for experimental measurements (Vahabli and Rahmati (2016b))

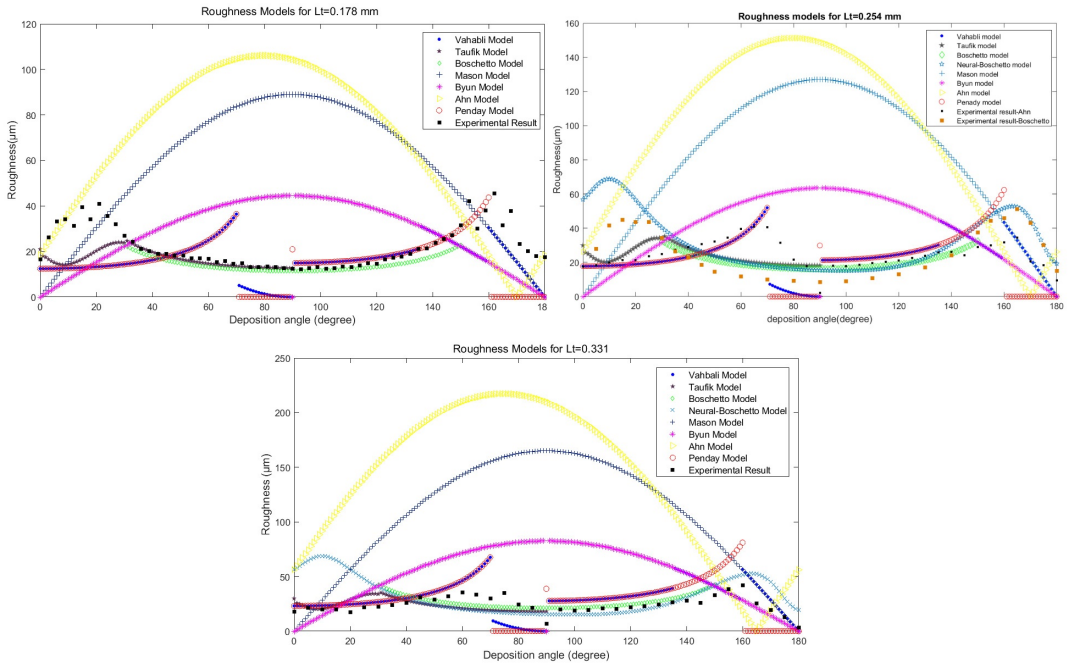

Figure 9. Roughness models and experimental data for $L_t = 0.178$,0.254, and 0.3301 mm

described for layer thickness of $L_t = 0.178, 0.254$, and 0.331 mm as shown in Figure 9.

As shown in Figure 9, the experimental data are illustrated by squares. For $L_t = 0.178$ mm, there are some models like the Boschetto model, Taufik model, and Penday model which seem efficient to predict the product roughness for some deposition angle ranges but they are not cover all the possible orientations. In this figure for $L_t = 0.254$ mm, these models are not able to predict the product roughness for all possible orientations. Also, it is illustrated that the models of Boschetto and Ahn do not correspond to their experimental data. Also, the figure related to $L_t = 0.331$ mm illustrates that these presented models do not correspond to experimental data for all possible values of deposition angle as orientation factor of product.

To conclude, there is no model that support the experimental data as illustrated in these figures. Therefore, it is essential to provide a novel model that will be developed based on the interpolation of experimental data as a meta-modeling approach in this study.

In the next section, a new roughness model for AM as our proposed methodology will be explained comprehensively.

4. New roughness model

To provide a generic new roughness model which can be used for all the layer thickness and deposition angle values, it is necessary to find the database to create the meta-model based on this data. For this purpose, the first step is to collect the appropriate data as follow:

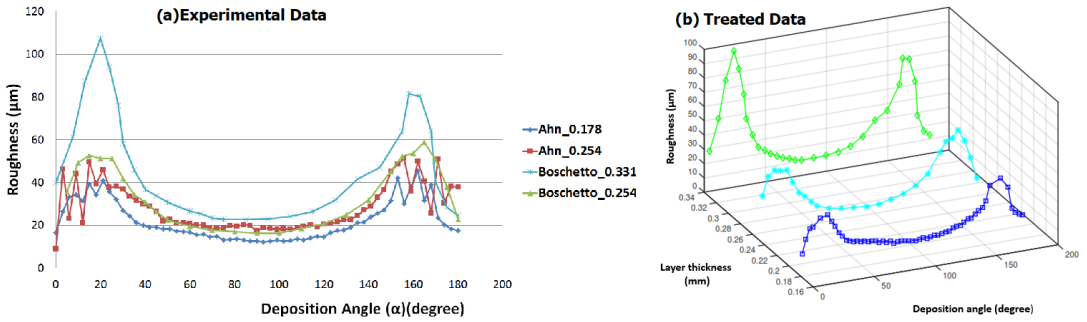

Figure 10. (a) Experimental data from Ahn and Boschetto roughness tests (b) Treated data of roughness experiments for different layers thicknesses

4.1. *Collecting the data:*

Analysis of different researches creates a possibility to gather the experimental data for the roughness value of the product fabricated on ABS (Acrylonitrile Butadiene Styrene). As summarized in Table 1, Ahn et al. (2009) and Boschetto, Giordano, and Veniali (2013a) performed the experiments on the specimens fabricated on ABS. As illustrated in Figure 10, Ahn presented the experimental data for layer thickness of 0.178 and 0.254 mm. Also, Boschetto performed the experiments which permit gathering the product roughness data for $L_t = 0.254$ and $L_t = 0.331$ mm. Therefore, these data are collected (see Figure 10 a) in this study to create a meta-model for roughness value based on two parameters of layer thickness and deposition angle.

To propose our meta-model, it is necessary to treat the data in order to have a robust model. For the angles, 0°, 25°, 155°, and 180°, the Ahn model presents oscillations which seem difficult to justify physically, whereas the Boschetto model gives a much more coherent response without any oscillations. Therefore, the experimental values obtained by Boschetto are supposed for these mentioned angles. Then, the mean values of data coming from Ahn and Boschetto are supposed for other angles as selected data. Therefore, this treated data for different layer thickness values are shown in Figure 10 b.

After finding the appropriate database, the meta-model can be explored as follow:

4.2. *Meta-model*

The data obtained by analyzing experimental data can be used to find a surface response or meta-model. There are several "families" of meta-models, including models based on polynomial functions (polynomials of degrees a few, RBF (Radial Basis Function), Krigeage, etc.) and models using a list of basic analytical functions (trigonometric functions, logarithmic functions, etc.) (Forrester, Sobester, and Keane (2008)). In this study, the second category is used to find the meta-model as its implementation is more simple and it used fewer coefficients than other techniques based on polynomial functions. Therefore, Genetic programming as a GPTIPS tool in Matlab is used to find the proposed model.

Genetic programming (GP) is a biologically inspired machine learning method for performing a task by computer programming (Koza and Koza (1992)). In this method, a random population is generated (represented by tree structures). Then, mutation and cross-over as genetic operators are used to find the best performing trees to create a

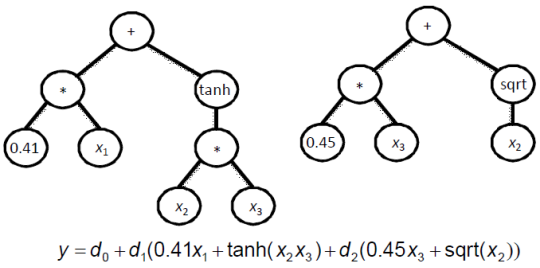

Figure 11. Example of a multi-gene symbolic model (Searson (2009))

new population. This process is repeated for the specified iteration until the population contains programs that solve the task well. The GP can be known as symbolic regression when the task is building an empirical mathematical model of data acquired from a process or system. Unlike traditional regression analysis (in which the user must specify the model structure), GP automatically evolves both the structure and the parameters of the mathematical model (Searson (2009)). This symbolic regression can be used in academic (Alfaro-Cid et al. (2009)) and industrial applications (Kordon (2006)).

GP is used in symbolic regression to evolve a population of trees. Each of these threes encodes a mathematical equation which predicts a $(N \times 1)$ vector of outputs y by using a corresponding $(N \times M)$ matrix of inputs X where N is the number of observations of the response variable and M is the number of input (predictor) variables. For example, the ith column of X consists of the N input values for the i^{th} input variable and may be designated as the input variable x_i (Searson (2009)). While in multi-gene symbolic regression, each symbolic model (and each member of the GP population) is a weighted linear combination of the outputs from several GP trees, where each tree is considered as a "gene". For instance, as shown in Figure 11, the multi-gene model predicts an output variable by using the input variables x_1, x_2, and x_3. The structure of this model contains non-linear terms (e.g. the hyperbolic tangent) but it is linear in the parameters with respect to the coefficients d_0, d_1 and d_2 (Searson (2009)). In this method, the maximum number of genes G_{max} and the maximum tree depth D_{max} are specified by the user which controls the maximum complexity of the evolved models. The linear coefficients of each model are estimated from the experimental data by using ordinary least squares techniques. Therefore, multi-gene GP combines the power of classical linear regression with the ability to capture non-linear behavior without needing to pre-specify the structure of the non-linear model (Searson (2009)).

The multi-gene symbolic regression is more accurate and computationally efficient than the standard GP approach for symbolic regression and it can be successfully embedded within a non-linear partial least squares algorithm (Hinchliffe et al. (1996); Searson (2009)). In the following, GPTIPS is described comprehensively:

- In GPTIPS, the initial population is constructed by creating individuals that contain randomly generated GP trees with between 1 and G_{max} genes. A gene is selected randomly from each parent individual, a standard sub-tree crossover is performed and the resulting trees replace the parent trees in the otherwise unaltered individual in the next generation.
- Genes are acquired and deleted using a tree crossover operator called a two-point

Table 2. GPTIPS algorithm parameters

Population size	200	Number of generation	500	Number of run	10
Tournament size	100	Tournament percentage of Pareto	0.4	Elite fraction	0.3
		Maximum iteration	500		

high-level crossover. This allows the exchange of genes between individuals and it is used in addition to the "standard" GP recombination operators. If the ith gene in an individual is labeled G_i then a two-point high-level crossover is performed. For example, the first parent individual contains the genes $(G_1G_2G_3)$ and the second one contains the genes $(G_4G_5G_6G_7)$ where $G_{max} = 5$. Two randomly selected crossover points are created for each individual. The genes enclosed by the crossover points are denoted by $< \ldots >$ as $((G_1 < G_2 > G_3)(G_4 < G_5G_6G_7 >))$. The genes enclosed by the crossover points are then exchanged resulting in the two new individuals $((G_1G_5 > G_6G_7G_3)(G_4G_2))$.

- Two-point high-level crossover permits not only the acquisition of new genes for both individuals but also removing the genes. Therefore, if an exchange of genes results in an individual containing more genes than G_{max} then genes are randomly selected and deleted until the individual contains G_{max} genes.
- GPTIPS provides several methods of mutating trees.
- The relative probabilities will be devoted to each recombination process. These processes are grouped as events. These events are mutation and crossover. The probabilities for the event are sub-types like the probability of two-point high-level crossover and sub-tree of mutation. However, GPTIPS provides the default values for each of these probabilities, so there is no need to be set by the user.
- Overall, GPTIPS contains the following configurable GP features: tournament selection and plain lexicographic tournament selection (Luke and Panait (2002)), elitism, three different tree-building methods (full, grow and ramped-half and a half), and six different mutation operators including sub-tree mutation, mutation of constants using an additive Gaussian perturbation, as well as substitution of a randomly selected input node with another randomly selected input node, set a randomly selected constant to zero, substitute a randomly selected constant with another randomly generated constant, and set a randomly selected constant to one.

Therefore, this GPTIPS method is used in this study to find the best fitness function of the surface roughness based on the experimental data. The best fitness is obtained through considering the parameters of the algorithm as shown in Table 2. This function is a mathematical formulation of roughness in terms of deposition angle and layer thickness. Therefore, Equation (15) illustrates the relation between layer thickness as L_t and deposition angle as α and surface roughness (R_a) as shown in Figure 12. This function is a prediction of surface roughness with a maximum gap of 3.93 µm. This gap is the maximum difference between the predicted model and the experimental data.

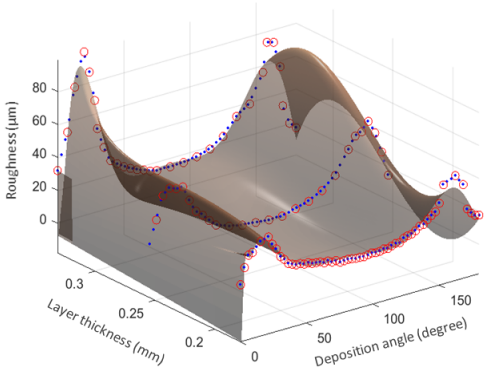

Figure 12. Surface roughness model

$$R_{\mathrm{a}} = 0.09309\,\mathrm{e}^{\sqrt{\alpha}} - 20.12L_t - 0.6626\,\mathrm{e}^{\sqrt{L_t\,\alpha}} - 49.08\,\alpha - 77.35\,\mathrm{e}^{0.0427\,\alpha} + 0.3953\,\mathrm{e}^{\mathrm{e}^{L_t}}$$
$$- 0.09309\,\mathrm{e}^{\alpha^{L_t}} + 2.915\ \times 10^{-5}\,\alpha^4\,{L_t}^2 + 34.64\,\alpha\,{L_t}^{L_t} + 0.1443\,\alpha^{L_t}\,\mathrm{e}^{0.0427\,\alpha} + 0.7036\,\alpha\,L_t$$
$$+0.2505\,\alpha\,\mathrm{e}^{0.0427\,\alpha} - 190.7\,{L_t}^{\alpha\,{L_t}^2} - 32.11\,\alpha^{L_t}\,\mathrm{e}^{L_t} + 4.919\,\sqrt{\mathrm{e}^{\sqrt{\alpha}}} - 3.945\,\sqrt{\alpha\,L_t} - 0.02231\,\alpha^{5/2}\,L_t$$
$$-83.18\,L_t\,\mathrm{e}^{L_t} - 5.232\,{L_t}^{3/2}\,\mathrm{e}^{0.0427\,\alpha} + 127.4\,\sqrt{L_t}^{\mathrm{e}^{0.0427\,\alpha}} + 0.1985\,\alpha^2 + 104.1\,\sqrt{\alpha} - 4.648\,\sqrt{L_t}$$
$$+63.68\,\sqrt{L_t}^{\mathrm{e}^{\alpha\,L_t}} + \frac{0.2525\,\alpha^2}{(\alpha\,L_t)^{1.0\,\alpha}} + 34.64\,\alpha\,L_t\,\mathrm{e}^{L_t} + 1.194\,\alpha^2\,{L_t}^{\alpha}\,\mathrm{e}^{\alpha} - 61.17\,\alpha^{L_t}\,\mathrm{e}^{L_t}\,\sqrt{\mathrm{e}^{L_t}} + 212.7 \tag{15}$$

4.3. *Discussions and results analysis*

The effect of this roughness value on the surface quality of the product is a significant challenge in the utilization of AM as a manufacturing technology in the industrial world. AM is a new technology that coming in the age of industry 4.0 which must be competitive with the other classic manufacturing methods due to its advantages like flexibility, ability to produce complex products, etc. Therefore, it is necessary not only to improve the AM features but also, to predict these features before production through estimation methodologies to have a cost-effective production. Therefore, a comprehensive analysis of different studies on surface roughness models is provided in this paper which permits to find a generic roughness model based on layer thickness and part orientation as the most significant factors for surface roughness.

To the best of our knowledge, no generic model is presented for predicting the surface roughness value which respects the experimental data. This study proposed a meta-model based on experimental data that permits researchers and manufacturers to quantify the surface quality before production. Also, this quantification helps the users to find the best or optimal values of the significant manufacturing parameters, as layer thickness and deposition angle, in order to create a production more cost-effective.

To illustrate the effectiveness of our proposed meta-model, the results obtained by this model is compared with the existed models and experimental data. As illustrate in Figure 13, these data are presented for the layer thickness of 0.178, 0.254, and 0.3302 mm. These comparisons illustrate that the proposed model is sufficiently

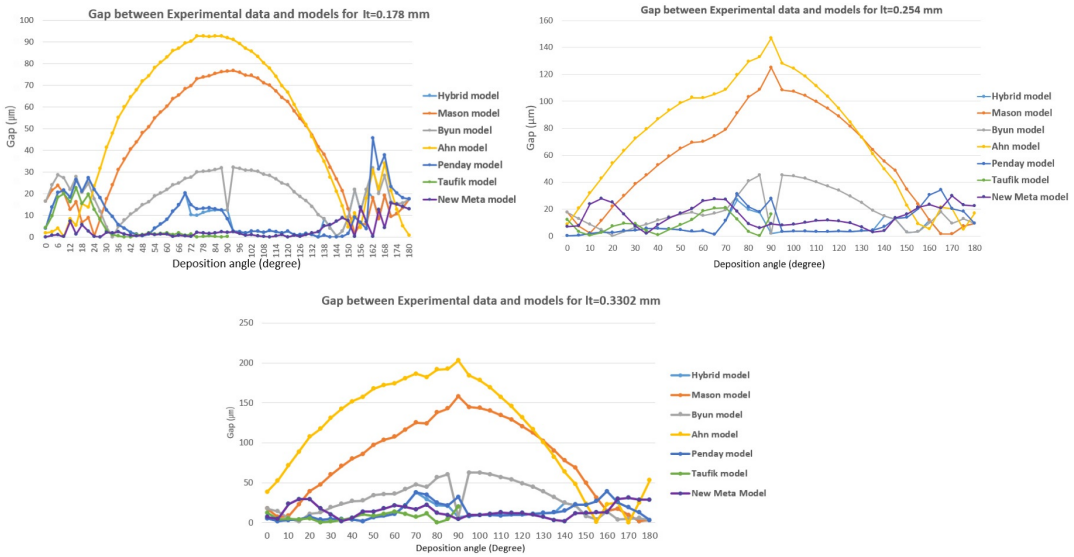

Figure 13. Gap between experimental data and different models

efficient to predict the product surface roughness before production.

According to this analysis, shown in Figure 14, the minimum and maximum prediction error are illustrated. This analysis shows that the minimum prediction error are for the layer thickness 0.178, 0.254, and 0.331 mm are respectively 0.065, 0.65, and 0.24 %. These maximum errors are 77 % for the layer thickness of 0.178 mm, and 110 % for the values of 0.254 and 0.331 mm. It is noteworthy to mention that for the small values of roughness in µm, these values can be negligible. Also, it can be concluded that this model is not very efficient for the values of more than 170°. To implement this model for a product and predict its roughness before production, a methodology is presented before by Asadollahi-Yazdi, Gardan, and Lafon (2018), to calculate the surface roughness for all facets of STL files in all possible orientations in the space and values of layer thickness.

5. Conclusions and Future works

This paper provides a comprehensive analysis of the surface quality of the FDM product as a major issue of fabrication with AM technologies. Different models including empirical and theoretical models are presented by other researchers but no model is reliable due to experimental data for predicting the surface quality of the produced product before fabrication. Therefore, a new model for roughness estimation is developed according to experimental data through a meta-modeling approach. Analyses of different studies provide a precondition to present a generic model that can be used to predict the surface roughness of the product before producing it or to optimize its geometry. This generic model permits to investigate surface roughness in design and fabrication of FDM products in order to apply an integrated design based on DfAM methodology.

The quality of this proposed meta-model depends on the experimental data. So, data robustness is a factor that can improve the proposed model. Providing an appropriate condition in terms of other AM parameters as temperature, fabrication speed, etc. for

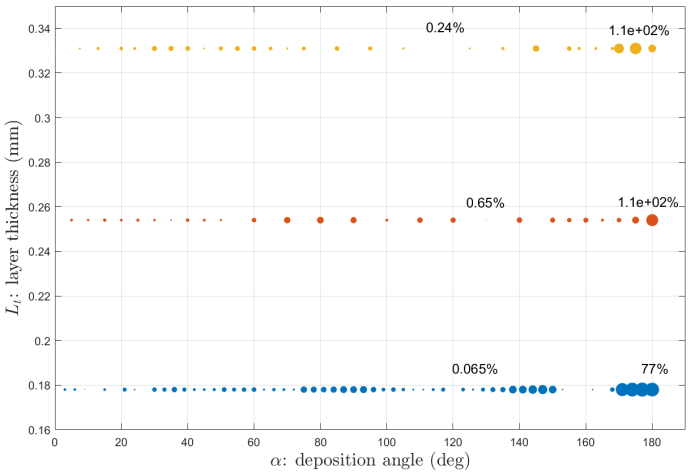

Figure 14. Prediction error based on layer thicknesses and deposition angles data

performing different experiments, as well as collecting more data help to present a more precise model.

For future works, this model will be used to find the optimal manufacturing parameters to minimize surface roughness. Also, different technologies need a prediction model for the roughness of AM products before fabrication to reduce time and cost, as well as improve the surface quality.

6. Acknowledgements

The authors gratefully acknowledge the Grand-Est region in France and the European Regional Development Fund (ERDF) for their financial supports.

References

Ahn, Dae-Keon, Soon-Man Kwon, and Seok-Hee Lee. 2008. "Expression for surface roughness distribution of FDM processed parts." In *Smart Manufacturing Application, 2008. ICSMA 2008. International Conference on*, 490–493. IEEE.

Ahn, Daekeon, Hochan Kim, and Seokhee Lee. 2009. "Surface roughness prediction using measured data and interpolation in layered manufacturing." *Journal of materials processing technology* 209 (2): 664–671.

Ahn, Daekeon, Jin-Hwe Kweon, Soonman Kwon, Jungil Song, and Seokhee Lee. 2009. "Representation of surface roughness in fused deposition modeling." *Journal of Materials Processing Technology* 209 (15): 5593–5600.

Alfaro-Cid, Eva, Anna I Esparcia-Alcázar, Pilar Moya, Beatriu Femenia-Ferrer, Ken Sharman, and JJ Merelo. 2009. "Modeling pheromone dispensers using genetic programming." In *Workshops on Applications of Evolutionary Computation*, 635–644. Springer.

Asadollahi-Yazdi, E, J Gardan, and P Lafon. 2016. "Integrated Design in Additive Manufacturing Based on Design for Manufacturing." *World Academy of Science, Engineering and Technology, International Journal of Mechanical, Aerospace, Industrial, Mechatronic and Manufacturing Engineering* 10 (6): 1137–1144.

Asadollahi-Yazdi, Elnaz, Paulin Couzon, Nhan Quy Nguyen, Yassine Ouazene, Farouk Yalaoui, et al. 2020. "Industry 4.0: Revolution or Evolution?" *American Journal of Operations Research* 10 (06): 241.

Asadollahi-Yazdi, Elnaz, Julien Gardan, and Pascal Lafon. 2017. "Integrated Design for Additive Manufacturing Based on Skin-Skeleton Approach." *Procedia CIRP* 60: 217–222.

Asadollahi-Yazdi, Elnaz, Julien Gardan, and Pascal Lafon. 2018. "Toward integrated design of additive manufacturing through a process development model and multi-objective optimization." *The International Journal of Advanced Manufacturing Technology* 1–20.

Boschetto, A, V Giordano, and F Veniali. 2013a. "Surface roughness prediction in fused deposition modelling by neural networks." *The International Journal of Advanced Manufacturing Technology* 67 (9-12): 2727–2742.

Boschetto, Alberto, Luana Bottini, and Francesco Veniali. 2016. "Finishing of Fused Deposition Modeling parts by CNC machining." *Robotics and Computer-Integrated Manufacturing* 41: 92–101.

Boschetto, Alberto, Veronica Giordano, and Francesco Veniali. 2013b. "3D roughness profile model in fused deposition modelling." *Rapid Prototyping Journal* 19 (4): 240–252.

Byun, Hong S, and Kwan H Lee. 2006. "Determination of optimal build direction in rapid prototyping with variable slicing." *The International Journal of Advanced Manufacturing Technology* 28 (3-4): 307.

Byun, Hong-Seok, and Kwan Heng Lee. 2003. "Design of a new test part for benchmarking the accuracy and surface finish of rapid prototyping processes." In *International Conference on Computational Science and Its Applications*, 731–740. Springer.

Cherkia, Hemant, Sasmita Kar, Sudhansu Sekhar Singh, and Ashutosh Satpathy. 2020. "Fused Deposition Modelling and Parametric Optimization of ABS-M30." In *Advances in Materials and Manufacturing Engineering*, 1–15. Springer.

Forrester, Alexander, Andras Sobester, and Andy Keane. 2008. *Engineering design via surrogate modelling: a practical guide*. John Wiley & Sons.

Gardan, Julien. 2016. "Additive manufacturing technologies: state of the art and trends." *International Journal of Production Research* 54 (10): 3118–3132.

Garg, Parlad Kumar, Rupinder Singh, and IPS Ahuja. 2017. "Multi-objective optimization of dimensional accuracy, surface roughness and hardness of hybrid investment cast components." *Rapid Prototyping Journal* 23 (5): 845–857.

Hinchliffe, MP, MJ Willis, H Hiden, MT Tham, B McKay, and GW Barton. 1996. "Modelling chemical process systems using a multi-gene genetic programming algorithm." In *Genetic Programming: Proceedings of the First Annual Conference (late breaking papers)*, 56–65.

Huang, Bai, Shuna Meng, Hui He, Yunchao Jia, Yingbin Xu, and Huankun Huang. 2019. "Study of processing parameters in fused deposition modeling based on mechanical properties of acrylonitrile-butadiene-styrene filament." *Polymer Engineering & Science* 59 (1): 120–128.

Jain, Rajat, Shivansh Nauriyal, Vishal Gupta, and Kanwaljit Singh Khas. 2020. "Effects of Process Parameters on Surface Roughness, Dimensional Accuracy and Printing Time in 3D Printing." In *Advances in Production and Industrial Engineering*, 187–197. Springer.

Jayanth, N, P Senthil, and C Prakash. 2018. "Effect of chemical treatment on tensile strength and surface roughness of 3D-printed ABS using the FDM process." *Virtual and Physical Prototyping* 13 (3): 155–163.

Khan, MS, and JP Dash. 2019. "Enhancing Surface Finish of Fused Deposition Modelling Parts." In *3D Printing and Additive Manufacturing Technologies*, 45–57. Springer.

Ko, Sukjin, and Donghun Lee. 2017. "Stiffness optimization of 5-axis machine tool for improving surface roughness of 3D printed products." *Journal of Mechanical Science and Technology* 31 (7): 3355–3369.

Kordon, Arthur K. 2006. "Future trends in soft computing industrial applications." In *2006 IEEE International Conference on Fuzzy Systems*, 1663–1670. IEEE.

Koza, John R, and John R Koza. 1992. *Genetic programming: on the programming of computers by means of natural selection*. Vol. 1. MIT press.

Lalegani Dezaki, Mohammadreza, Mohd Khairol Anuar Mohd Ariffin, and Mohd Idris Shah Ismail. 2020. "Effects of CNC Machining on Surface Roughness in Fused Deposition Modelling (FDM) Products." *Materials* 13 (11): 2608.

Li, Aijun, Zhuohui Zhang, Daoming Wang, and Jinyong Yang. 2010. "Optimization method to fabrication orientation of parts in fused deposition modeling rapid prototyping." In *Mechanic Automation and Control Engineering (MACE), 2010 International Conference on*, 416–419. IEEE.

Li, Hongbin, Taiyong Wang, Jian Sun, and Zhiqiang Yu. 2016. "The adaptive slicing algorithm and its impact on the mechanical property and surface roughness of freeform extrusion parts." *Virtual and Physical Prototyping* 11 (1): 27–39.

Luke, Sean, and Liviu Panait. 2002. "Lexicographic parsimony pressure." In *Proceedings of the 4th Annual Conference on Genetic and Evolutionary Computation*, 829–836. Morgan Kaufmann Publishers Inc.

Mason, Andrew. 2006. "Multi-axis hybrid rapid prototyping using fusion deposition modeling." .

Mu, Mulan, Chun-Yen Ou, Junjie Wang, and Yongliang Liu. 2020. "Surface modification of prototypes in fused filament fabrication using chemical vapour smoothing." *Additive Manufacturing* 31: 100972.

Nagendra, J, MK Srinath, S Sujeeth, KS Naresh, and MS Ganesha Prasad. 2020. "Optimization of process parameters and evaluation of surface roughness for 3D printed nylon-aramid composite." *Materials Today: Proceedings* .

Pandey, PM, N Venkata Reddy, and SG Dhande. 2003a. "Real time adaptive slicing for fused deposition modelling." *International Journal of Machine Tools and Manufacture* 43 (1): 61–71.

Pandey, PM, N Venkata Reddy, and SG Dhande. 2007. "Part deposition orientation studies in layered manufacturing." *Journal of materials processing technology* 185 (1-3): 125–131.

Pandey, PM, NV Reddy, and SG Dhande. 2003b. "Surface roughness simulation for FDM processed parts." In *Proceedings of 18th International Conference on Computer Aided Production Engineering*, Vol. 44, 413–421.

Pandey, Pulak M, N Venkata Reddy, and Sanjay G Dhande. 2003c. "Improvement of surface finish by staircase machining in fused deposition modeling." *Journal of materials processing technology* 132 (1): 323–331.

Pandey, Pulak M, K Thrimurthulu, and N Venkata Reddy*. 2004. "Optimal part deposition orientation in FDM by using a multicriteria genetic algorithm." *International Journal of Production Research* 42 (19): 4069–4089.

Pérez, Mercedes, Gustavo Medina-Sánchez, Alberto García-Collado, Munish Gupta, and Diego Carou. 2018. "Surface quality enhancement of fused deposition modeling (FDM) printed samples based on the selection of critical printing parameters." *Materials* 11 (8): 1382.

Rajan, A John, M Sugavaneswaran, B Prashanthi, Siddhant Deshmukh, and S Jose. 2020. "Influence of Vapour Smoothing Process Parameters on Fused Deposition Modelling Parts Surface Roughness at Different Build Orientation." *Materials Today: Proceedings* 22: 2772–2778.

Reddy, NV, and Pulak M Pandey. 2005. "Enhancement of surface finish in Fused Deposition Modelling." In *Virtual Modelling and Rapid Manufacturing: Advanced Research in Virtual and Rapid Prototyping Proc. 2nd Int. Conf. on Advanced Research in Virtual and Rapid Prototyping, 28 Sep-1 Oct 2005, Leiria, Portugal*, 461. CRC Press.

Salokhe, Omkar A, and Aamir M Shaikh. 2019. "Study of Fused Deposition Modeling Process Parameters for Polycarbonate/Acrylonitrile Butadiene Styrene Blend Material using Taguchi Method." .

Searson, Dominic. 2009. "GPTIPS genetic programming & symbolic regression for MATLAB user guide." .

Sheoran, Ankita Jaisingh, and Harish Kumar. 2019. "Fused Deposition modeling process parameters optimization and effect on mechanical properties and part quality: Review and reflection on present research." *Materials Today: Proceedings* .

Singh, Daljinder, Rupinder Singh, and KS Boparai. 2020. "Investigations for surface roughness and dimensional accuracy of biomedical implants prepared by combining fused deposition modelling, vapour smoothing and investment casting." *Advances in Materials and Processing Technologies* 1–20.

Sreedhar, P., Manikandan C. Mathikumar, and G. Jothi. 2012. "Experimental investigation of surface roughness for fused deposition modeled part with different angular orientation." .

Standard, ASME. 2002. "B46. 1 (2002) Surface Texture, Surface Roughness, Waviness and Lay." *American Society of Mechanical Engineers, New York, NY* .

Taufik, Mohammad, and Prashant K Jain. 2016. "A study of build edge profile for prediction of surface roughness in fused deposition modeling." *Journal of Manufacturing Science and Engineering* 138 (6): 061002.

Thrimurthulu, K, Pulak M Pandey, and N Venkata Reddy. 2004. "Optimum part deposition orientation in fused deposition modeling." *International Journal of Machine Tools and Manufacture* 44 (6): 585–594.

Vahabli, Ebrahim, and Sadegh Rahmati. 2016a. "Application of an RBF neural network for FDM parts' surface roughness prediction for enhancing surface quality." *International journal of precision engineering and manufacturing* 17 (12): 1589–1603.

Vahabli, Ebrahim, and Sadegh Rahmati. 2016b. "Hybrid estimation of surface roughness distribution in FDM parts using analytical modeling and empirical investigation." *The International Journal of Advanced Manufacturing Technology* 5 (88): 2287–2303.

Vaneker, Tom, Alain Bernard, Giovanni Moroni, Ian Gibson, and Yicha Zhang. 2020. "Design for additive manufacturing: Framework and methodology." *CIRP Annals* 69 (2): 578–599.

Wang, Peng, Bin Zou, Hongchuan Xiao, Shouling Ding, and Chuanzhen Huang. 2019. "Effects of printing parameters of fused deposition modeling on mechanical properties, surface quality, and microstructure of PEEK." *Journal of Materials Processing Technology* .